The Strength of Dehalogenase−Substrate Hydrogen Bonding Correlates with the Rate of Meisenheimer Intermediate Formation†

Jian Dong,‡ Xuefeng Lu,§ Yansheng Wei,§ Lusong Luo,§ Debra Dunaway-Mariano,*,§ and Paul R. Carey*,‡

Department of Biochemistry, Case Western Reserve University, 10900 Euclid Avenue, Cleveland, Ohio 44106-4935, and Department of Chemistry, University of New Mexico, Albuquerque, New Mexico 87131

Received May 20, 2003; Revised Manuscript Received June 11, 2003

ABSTRACT: 4-Chlorobenzoyl-coenzyme A (4-CBA-CoA) dehalogenase catalyzes the hydrolytic dehalogenation of 4-CBA-CoA to 4-hydroxybenzoyl-CoA by using an active site aspartate as the nucleophile. Formation of the corresponding Meisenheimer complex (EMc) is followed by chloride ion expulsion which forms the arylated intermediate (EAr). This is then hydrolyzed to the product. In this paper, we explore the relationship between active site polarizing forces acting on the benzoyl carbonyl and the rate of formation of the Meisenheimer complex. The polarizing forces at the C═O group were modulated by introducing site-selected mutations (A112V, Y65D, G113A, G113S, G113N, and F64P), near the C═O binding site. Using either the substrate, 4-CBA-CoA, or the substrate analogue, 4-methylbenzoyl-CoA (4-MBA-CoA), Raman difference spectroscopy provided the position of the C═O stretching frequency ($\nu_{C=O}$) for a total of 10 enzyme−ligand complexes. In turn, the values of the C═O frequencies could be converted to differences in effective hydrogen bonding strengths between members of the series, based on earlier model studies [Clarkson, J., Tonge, P. J., Taylor, K. L., Dunaway-Mariano, D., and Carey, P. (1997) *Biochemistry 36*, 10192−10199]. Catalysis in the F64P, G113A, G113S, and G113N dehalogenase mutants was very slow with k_{cat} values ranging from 8×10^{-3} to 7.6×10^{-6} s^{-1}. The EAr intermediate did not accumulate to a detectable level on these enzymes during a single turnover. Catalysis in the Y65D and A112V dehalogenase mutants were almost as efficient as catalysis in wild-type dehalogenase with k_{cat} values of 0.1−0.6 s^{-1}. In wild-type dehalogenase, 22% of the bound substrate accumulated as the EAr intermediate during a single turnover (k_{obs} for EAr formation = 24 s^{-1}); in the Y65D mutant, the level of accumulation is 17% (k_{obs} for EAr formation = 3 s^{-1}), and in the A112V mutant, the level is 23% (k_{obs} for EAr formation = 17 s^{-1}). The k_{obs} for EAr formation in wild-type dehalogenase and the more active dehalogenase mutants (Y65D and A112V) was taken to be an estimate of the *k* for EMc formation, and the k_{obs} for EP formation in a single turnover was taken to be an estimate of the *k* for EMc formation in the severely impaired mutants (F64P, G113A, G113S, and G113N). A plot of the log k_{obs} for EMc formation versus the C═O stretching frequency of bound 4-CBA-CoA (or 4-MBA-CoA) is a straight line ($R^2 = 0.9584$). Throughout the series, $\nu_{C=O}$ varied by 61 cm^{-1}, corresponding to the change in hydrogen bonding enthalpy of 67 kJ/mol. The results show that changes in polarizing forces at the benzoyl carbonyl are transmitted to the benzoyl (4) position and correlate with the rate of aromatic nucleophilic addition five chemical bonds away. Interestingly, the relationship between effective polarizing forces and reactivity seen here for dehalogenase is similar to that reported for the addition−elimination reaction involving the hydrolysis of a series of acyl serine proteases.

In an environment as complex as an enzyme's active site, it would be of great interest to assess the interactions between individual enzyme and substrate groups and to determine the effect of these interactions on reactivity. For most enzymes, this goal is beyond reach, but the system presented here, involving the hydrolytic dehalogenation of 4-chlorobenzoyl-coenzyme A (4-CBA-CoA)[1] by a dehalogenase, offers an unusual opportunity to explore just such a relationship. Selected mutations have been employed to vary the strength of the hydrogen bonds to the substrate's benzoyl carbonyl, and using Raman spectroscopy, it is possible to quantitate the changes in hydrogen bond enthalpy at the C═

† This research was supported by NIH Grants GM-28688 (to D.D.-M.) and GM-54072 (to P.R.C.).

* To whom correspondence should be addressed. P.R.C.: phone, (216) 368-0031; fax, (216) 368-3419; e-mail, carey@biochemistry.cwru.edu. D.D.-M.: phone, (505) 277-3383; fax, (505) 277-6202; e-mail, dd39@unm.edu.

‡ Case Western Reserve University.

§ University of New Mexico.

[1] Abbreviations: 4-CBA, 4-chlorobenzoate; 4-CBA-CoA, 4-chlorobenzoyl-coenzyme A; 4-HBA-CoA, 4-hydroxybenzoyl-CoA; 4-MBA-CoA, 4-methylbenzoyl-CoA; Hepes, *N*-(2-hydroxyethyl)piperazine-*N*′-2-ethanesulfonic acid; Tris, tris(hydroxymethyl)aminomethane; DTT, dithiothreitol; WT, wild-type; ES, dehalogenase−4-CBA-CoA complex; EP, dehalogenase−4-HBA-CoA complex; EMc, Meisenheimer complex (σ-complex) formed by addition of the dehalogenase Asp145 to C(4) of the substrate benzoyl; EAr, benzoyl-CoA ester formed with the dehalogenase active site Asp145; S_NAr, aromatic nucleophilic substitution; H-bond, hydrogen bond.

10.1021/bi0347656 CCC: $25.00
Published on Web 07/15/2003

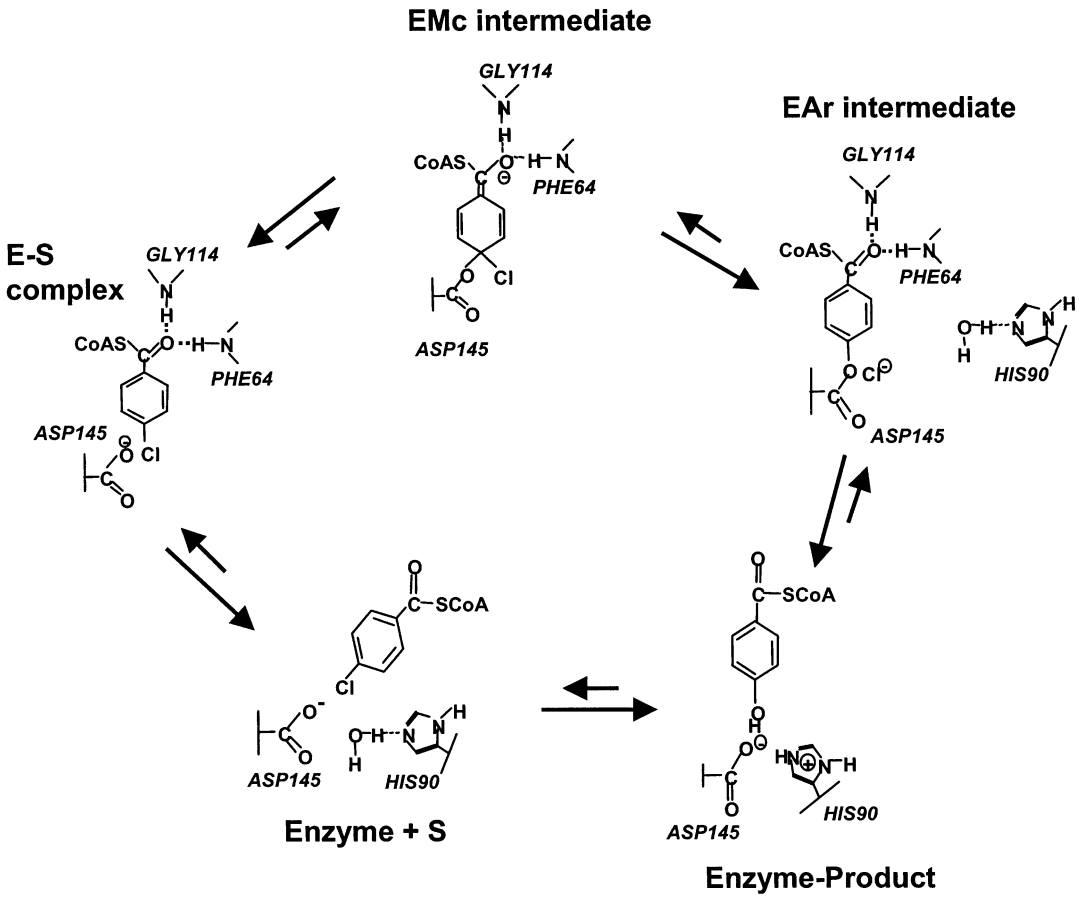

FIGURE 1: *Pseudomonas* sp. strain CBS-3 4-CBA-CoA dehalogenase-catalyzed conversion of 4-CBA-CoA to 4-HBA-CoA.

O group. It is found that these changes correlate with rate of formation of the first intermediate on the reaction pathway, a Meisenheimer complex.

4-CBA-CoA dehalogenase catalyzes the hydrolytic dehalogenation of 4-CBA-CoA to 4-hydroxybenzoyl-CoA (4-HBA-CoA) via a multistep mechanism involving initial attack of Asp145 on C(4) of the substrate benzoyl ring which forms a Meisenheimer intermediate (EMc) (*1*), followed by expulsion of the chloride ion which forms an arylated enzyme intermediate (EAr) and then ester hydrolysis in the EAr which forms the product (Figure 1) (*2*). The benzoyl C═O group of the bound substrate is positioned for H-bonding to the backbone amide NH groups of Phe64 and Gly114 and for electrostatic interaction with the positive pole of the α-helix of residues 114−122, while the benzoyl ring itself is surrounded by the aromatic rings of Phe64, Phe82, Trp89, and Trp137 (*3*). The rings provide a low-dielectric insulating sheath that probably facilitates the transmission of electronic effects through the benzoyl π-electron system. A major objective in this study is to search for a possible relationship linking interactions at the benzoyl C═O group with the rate of nucleophilic addition at benzoyl's C(4) position, five chemical bonds away.

In an earlier study, we impaired the interaction between the benzoyl C═O group and the electropositive sites on the enzyme by replacement of the C═O group with the C═S group (*4*). Raman difference spectroscopic studies of 4-HBA-dithio-CoA complexed to wild-type dehalogenase have shown that the C═S group does not transmit the electron pulling forces of the Gly114 and Phe64 backbone amide NH groups (*5*). Consequently, the dithio substrate analogue is less active as a substrate than 4-CBA-CoA, for example, with k_{cat} values of 3.2×10^{-3} and 0.6 s^{-1}, respectively.

In this work, we employ a different strategy to modulate the interaction between the benzoyl C═O and the electropositive sites on the enzyme; we modify the electropositive sites themselves. We have prepared and evaluated a series of site-directed mutants in which amino acid replacements were introduced at the A112, G113, and G115 positions flanking the α-helix N-terminus and at the G63 and Y65 positions flanking residue F64. As can be seen in Figure 2, these residues are near the C═O binding site, and thus, mutations at these sites are expected to cause subtle conformational changes that translate into a reduction in the strength of the electrostatic interaction with the substrate C═O group. Such a reduction would, in turn, result in a reduced level of polarization of the C═O group. This is measured by Raman difference spectroscopy and can be used to calculate the change in hydrogen bonding enthalpy. At the same time, the changed polarizing effects at the C═O group are transmitted to the 4 position of the benzoyl ring, bringing about changes in the rate of Meisenheimer complex formation. In this study, we show that there is a correlation between the effective hydrogen bonding strength at the benzoyl C═O group and the logarithm of the rate of formation of the Meisenheimer complex. Surprisingly, the relationship between the thermodynamic and kinetic parameters uncovered here bears a strong resemblance to that found for the deacylation behavior of a series of acyl serine proteases (*6*).

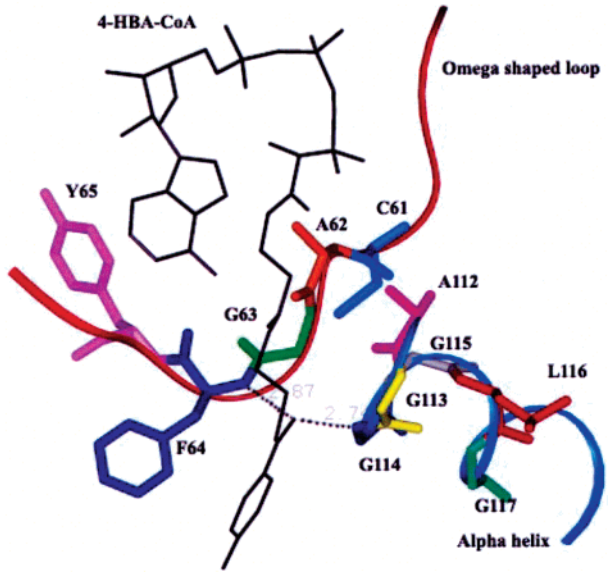

FIGURE 2: Target residues of mutation around the backbone NH group of G114 and F64 which perturb the function of the oxyanion hole in the wild-type 4-CBA-CoA dehalogenase (based on ref *3*). Black sticks denote the product 4-HBA-CoA. Dotted lines represent H-bonding interactions between the benzoyl C=O group and backbone amide NH groups of Phe64 and Gly114. An identical crystal structure with no conformational changes was also found for the 4-HBA-CoA−D145A mutant complex.

EXPERIMENTAL PROCEDURES

Materials

Ligands. 4-CBA-CoA, 4-MBA-CoA, and 4-HBA-CoA were prepared according to published procedures (*7*).

Enzymes. QuickChange mutagenesis (Stratagene) was used in combination with the *Sma*I−*Sal*I−pT7.5 plasmid (containing the 4-CBA-CoA dehalogenase gene) as a template (*8*) and the *Escherichia coli* BL21(DE3) cell line for construction of site-directed mutants. Mutant sequences were confirmed by DNA sequencing. Wild-type and mutant dehalogenases were purified according to the following procedure. BL21(DE3) cells transformed with WT (*8*) or mutant dehalogenase-encoding plasmid were grown at 28 °C in 3 × 2 L of LB medium containing 50 μg/mL ampicillin. Protein production was induced with 0.4 mM isopropyl β-D-galactopyranoside (IPTG) ca. 10 h postinoculation (cell density had reached an OD_{600} of 1.0). After a 5 h induction period, the cells were harvested by centrifugation (5000*g* for 15 min) and then suspended in 300 mL of buffer [50 mM K^+Hepes and 1 mM DTT (pH 7.5)] at 0 °C. The cell suspension was passed through a French press at 1200 psi and then centrifuged at 48000*g* and 4 °C for 1 h. The supernatant was chromatographed on a 40 cm × 15 cm DEAE-cellulose column [equilibrated with 50 mM K^+Hepes and 1 mM DTT (pH 7.5)] at 4 °C using a 1.5 L linear gradient from 0 to 0.35 M KCl in 50 mM K^+Hepes and 1 mM DTT (pH 7.5) as the eluant. The column fractions were analyzed by SDS−PAGE. The desired protein eluted at 0.1 M KCl. Solid $(NH_4)_2SO_4$ was added to the combined fractions to a final concentration of 10% (w/v). The resulting solution was chromatographed at 4 °C on a 18 cm × 3 cm Butyl-Sepharose column [pre-equilibrated with 10% (w/v) $(NH_4)_2SO_4$ in 50 mM K^+Hepes and 1 mM DTT (pH 7.5)]. The column was eluted with a 500 mL linear gradient from 10 to 0% $(NH_4)_2SO_4$ in 50 mM K^+Hepes and 1 mM DTT (pH 7.5). The desired protein fractions [eluted at ~5% $(NH_4)_2SO_4$] were combined and dialyzed in 50 mM K^+Hepes and 1 mM DTT (pH 7.5) for 4 h at 4 °C [to remove $(NH_4)_2SO_4$ present in the protein sample] prior to being loaded onto a 12 cm × 3 cm hydroxyapatite column [pre-equilibrated with 50 mM K^+Hepes and 1 mM DTT (pH 7.5)]. The column was eluted at 4 °C with a 400 mL linear gradient from 0 to 0.2 M $K_2^+(HPO_4)$ in 50 mM K^+Hepes and 1 mM DTT (pH 7.5). The purified protein (eluted at ~0.05 M potassium phosphate) was concentrated using an Amicon device (10 kDa Disc membrane) or a 10 kDa Macrosep centricon. (The hydroxyapatite chromatographic step is necessary for the removal of traces of a contaminating thioesterase activity.) The protein purity was confirmed by SDS−PAGE. The protein concentration was determined by using the Bradford method (*9*) and by the protein absorbance at 280 nm (extinction coefficient = 40 090 M^{-1} cm^{-1}). The yields were as follows: 15 mg/g (wet cell) for WT, 10 mg/g for G113A and G113S, 5 mg/g for Y65D, F64P, and G113N, 3 mg/g for A112V and A112S, and 1 mg/g for G113V and G115A.

Kinetic Assays

Steady-State Continuous Spectrophotometric Assay. This assay was used to measure k_{cat}, K_m, and K_i values for wild-type dehalogenase and k_{cat} and K_m values for the Y65D and A112V dehalogenase mutants. The initial velocity of the dehalogenase-catalyzed conversion of 4-CBA-CoA to 4-HBA-CoA was measured by monitoring the increase in solution absorption at 300 nm ($\Delta\epsilon$ = 8200 M^{-1} cm^{-1}). Reactions were carried out in 50 mM K^+Hepes (pH 7.5 and 25 °C) that contained wild-type (0.03 μM) or mutant dehalogenase (0.03 μM for Y65D and 0.08 μM for A112V) and varying concentrations of 4-CBA-CoA (0.5−10-fold greater than K_m). The initial velocity data were analyzed using eq 1 and the computer program KinetAsyst (IntelliKinetics) to calculate V_m and K_m. The k_{cat} was calculated from the ratio of V_m and enzyme concentration.

$$V = V_{max}[S]/([S] + K_m) \quad (1)$$

where V is the initial velocity, V_{max} the maximum velocity, [S] the substrate concentration, and K_m the Michaelis constant.

Steady-State Fixed-Time Assay. The K_m and/or k_{cat} values for the low-activity dehalogenase mutants G113A, G113S, G113N, and F64P were determined by measuring the amount of 4-HBA-CoA (at 330 nm, ϵ = 18 200 M^{-1} cm^{-1} for the 4-HBA-CoA phenoxide anion) formed in reaction mixtures incubated for a specific time period, and then quenched with base (110 μL of 0.3 M KOH added to 110 μL of reaction mixture). Reactions were carried out in 50 mM K^+Hepes (pH 7.5 and 25 °C) which contained 2 μM G113A, 5 μM G113S, 20 μM G113N, or 20 μM F64P dehalogenase and varying concentrations of 4-CBA-CoA (15−200 μM) (for G113A and G113S mutants) or a saturating concentration of 4-CBA-CoA (500 μM) (for F64P and G113N mutants). Reactions were terminated at or below 10% conversion of substrate. The initial velocity of the reaction was calculated from the slope of a plot of product concentration versus reaction time. Initial velocity data measured as a function

of 4-CBA-CoA concentration were analyzed by using eq 1 for calculation of V_m and K_m. The k_{cat} values for the G113N and F64P mutants were estimated from the ratio of the initial velocity measured at saturating 4-CBA-CoA concentrations and the enzyme concentration.

Single-Turnover Reactions Monitored by Stopped-Flow Absorption. Equal volumes (50 μL) of 40 μM 4-CBA-CoA and 120 μM dehalogenase mutant (Y65D and A112V) in 50 mM K^+Hepes (pH 7.5 and 25 °C) were mixed with a DX.17 MV stopped-flow spectrometer (Applied Photophysics, Leatherhead, U.K.) equipped with a 150 W xenon lamp (6 mm slit width). Data acquisition and processing were carried out with a 32-bit processor Archimedes workstation, which was also used for subsequent nonlinear regression analysis of the kinetic traces. The absorbance traces were measured at 370 nm (the molar extinction coefficient for the dehalogenase−4-HBA-CoA complex is in the range of 10000−17000 M^{-1} cm^{-1}, depending on the mutant used; the dehalogenase−4-CBA-CoA complex does not absorb at this wavelength) and were analyzed with a single-exponential equation (eq 2) to obtain the observed rate constant k_{obs}.

$$A_t = A_{max}[1 - \exp(-tk_{obs})] \quad (2)$$

where A_t is the absorbance at time t, A_{max} the maximal absorbance, and k_{obs} the apparent first-order rate constant.

The 370 nm absorption traces for reactions catalyzed by the low-activity dehalogenase mutants G113A and G113S were measured using a Beckman DU640 UV−vis spectrophotometer, following the hand mixing of enzyme and substrate.

Single-Turnover Reactions by Rapid Quenching or Hand Quenching. Single-turnover reactions catalyzed by wild-type dehalogenase and the Y65D and A112V mutant dehalogenases were monitored by measuring the amount of 4-HBA-CoA released from the enzyme upon denaturation (acid quench) and the amount of 4-HBA-CoA released from the precipitated enzyme fraction [arylated enzyme form (EAr)] upon base-catalyzed hydrolysis. A KINTEK rapid quench apparatus was used to mix 32 μL of 101 μM 4-CBA-CoA and 30 μL of 239 μM enzyme in 50 mM K^+Hepes (pH 7.5 and 25 °C). After a specified period of time, the reaction was quenched by the addition of 182 μL of 0.32 M HCl. A 200 μL aliquot was removed and mixed with 34 μL of 2.5 M KOH. The absorbance of the resulting solution was measured at 330 nm immediately after mixing. This absorbance was used to calculate the total amount of EAr and 4-HBA-CoA formed in the reaction. To measure the amount of EAr, 40 μL of saturated 4 M KCl was added to 244 μL of the acid-quenched reaction mixture to facilitate enzyme precipitation. The mixture was centrifuged with a NANOSEP 0.2 μm centrifugal concentrator. A 220 μL aliquot of the filtrate was mixed with 34 μL of 2.5 M KOH, and the absorbance of the resulting solution at 330 nm was measured (this step measures the amount of 4-HBA-CoA present in the quenched reaction mixture). The enzyme precipitant contained in the concentrator was suspended in 250 μL of 0.2 M HCl, which also contained 0.56 M KCl, and then centrifuged. This cycle was repeated twice more. The washed enzyme precipitant was then dissolved in 230 μL of 0.15 M KOH and centrifuged for 2 min in a NANOSEP 0.2 μm centrifugal concentrator. The absorbance of the filtrate at 330 nm was measured to determine the amount of 4-HBA-CoA generated from the hydrolysis of the arylated enzyme. For the reactions catalyzed by the low-activity dehalogenase mutants (F64P, G113A, G113S, and G113N), 250 μL reaction solutions [initially containing 60 μM dehalogenase mutant and 20 μM 4-CBA-CoA in 50 mM K^+Hepes (pH 7.5 and 25 °C)] were mixed by hand with 10 μL of 6 M HCl and 40 μL of saturated KCl. The reaction mixtures were separated and analyzed as previously described. The plots of EAr concentration versus reaction time were fitted using eq 2 to define the k_{obs} for EAr formation.

Ligand Dissociation Constants Measured by Fluorescence Titration. A FluoroMax-2 fluorometer was used in protein fluorescence quenching experiments aimed at measuring the binding constants of 4-MBA-CoA with wild-type and mutant dehalogenases. The intrinsic fluorescence spectrum of the dehalogenase (1 μM) in 50 mM K^+Hepes (pH 7.5 and 25 °C) that results from 290 nm excitation has an emission wavelength maximum at 337 nm. For a typical titration experiment, 1 μL aliquots of ligand were added to a 1 mL solution of 1 μM dehalogenase, and the fluorescence intensity at 337 nm was monitored. Because of filtration effects, the maximum ligand concentration that was used did not exceed 200 μM. Thus, for mutant−ligand pairs having large K_d values (<50 μM), titrations were carried out to partial saturation. The fluorescence data were fitted to eq 3 using the Kaleida Graph computer program for nonlinear regression analysis (*10*).

$$\Delta F/F_0 = [\Delta F_{max}/F_0([E])][K_d + [E] + [S] - \sqrt{(K_d + [E] + [S])^2 - 4[E][S]}]/2 \quad (3)$$

where [S] is the total ligand concentration, [E] the total enzyme concentration, K_d the apparent dissociation constant of the enzyme−ligand complex, F_{obs} the observed change in fluorescence intensity, F_{max} the maximum change in fluoresence intensity, and F_o the initial fluorescence intensity.

Raman Spectroscopy

The nonresonant Raman spectra were obtained using 647.1 nm laser excitation from an Innova 400 krypton laser system (Coherent, Inc.), a back-illuminated charge-coupled devise (CCD) detector (model 1024EHRB/1, Princeton Instruments, Inc.) operating at 183 K, and a Holospec f/1.4 axial transmission spectrometer (Kaiser Optical Systems, Inc.) employed as a single monochromator, as described in a previous report (*11*). Enzyme samples contained in cuvettes (50 μL in volume) were brought to appropriate concentrations and buffered with 50 mM Tris-HCl at pH 7.5. Enzyme and 4-CBA-CoA or 4-MBA-CoA concentrations that were used are given in the figure legends. Data were collected immediately after the complex had been made, using a laser power of ~950 mW and CCD exposure times of 5 min. The Raman spectrum of the buffer was subtracted from that of the ligand in buffer (giving the spectrum of the free ligand), while the spectrum of the enzyme in buffer was subtracted from that of the enzyme−ligand complex to give the spectrum of the bound ligand.

RESULTS

Changes in Polarization at the C=O Group: Effective Hydrogen Bonding Strength. The stretching frequency of the

Table 1: Steady-State Kinetic Constants (k_{cat} and K_m) for Catalyzed Dehalogenation of 4-CBA-CoA, Observed Rate Constants (k_{obs}) for the Single-Turnover Reaction of 4-CBA-CoA to 4-HBA-CoA (or where noted to arylated enzyme EAr), Dissociation Constants (K_d) for Dehalogenase Complexes of 4-Methylbenzoyl-CoA (4-MBA-CoA), and Thioester C═O Stretch Frequencies ($\nu_{C=O}$) in Dehalogenase Complexes[a]

	wild-type	F64P	Y65D	G113A	G113S	G113N	A112V
k_{cat} (s^{-1})	0.60 ± 0.01[b]	7.6×10^{-6}[c]	0.44 ± 0.01[b]	$(8 \pm 1) \times 10^{-3}$[b,c]	$(4.5 \pm 0.3) \times 10^{-4}$[c]	4.6×10^{-5}[c]	0.130 ± 0.001[b]
K_m (μM)	3.7 ± 0.3[b]		11 ± 0.7[b]	26 ± 11[b,c]	62 ± 9[c]		6.6 ± 0.3[b]
k_{cat}/K_m (s^{-1} μM^{-1})	0.16[b]		0.039[b]	3.2×10^{-4}[b,c]	6.5×10^{-6}[c]		0.019[b]
k_{obs} (s^{-1})	24 ± 0.5 for EAr[e]	1.0×10^{-5} for EP[f]	3.4 ± 0.9 for EAr[e]	$(4.5 \pm 0.04) \times 10^{-3}$ for EP[f]	$(8.5 \pm 0.9) \times 10^{-4}$ for EP[f]	3.9×10^{-5} for EP[f]	17 ± 0.5 for EAr[e]
	2.3 ± 0.1 for EP[d]		1.030 ± 0.006 for EP[d]				1.80 ± 0.02 for EP[d]
K_d (μM)[h]	1.6 ± 0.2	19 ± 4	1.7 ± 0.3	25 ± 4	140 ± 10	105 ± 30	2.5 ± 0.4
$\nu_{C=O}$ frequency (cm^{-1})	1608 (with D145A)[g]	1667[g]			1639[g]	1669[g]	
	1612[h]	1668[h]	1613[h]	1638[h]	1655[h]		1612[h]

[a] Reactions were carried out at pH 7.5 and 25 °C. See Experimental Procedures for details. [b] Measured by a steady-state continuous 300 nm spectrophotometric assay. [c] Measured by a steady-state fixed-time 330 nm spectrophotometric assay. [d] Measured by a single-turnover stopped-flow 370 nm spectrophotometric assay. [e] Measured by a single-turnover rapid quench 330 nm spectrophotometric assay. [f] Measured by a single-turnover hand quench 330 nm spectrophotometric assay. [g] Measured with the 4-CBA-CoA complex. [h] Measured with the 4-MBA-CoA complex.

thioester C═O bond for the bound ligand was measured by Raman difference spectroscopy (*11*−*13*). The wavelength of the excitation laser source was 647.1 nm, far from absorption bands of the benzoyl moiety of the ligands that occur near 280 nm. Thus, the experiments were carried out under nonresonance conditions, eliminating the possibility of photochemical changes being induced by the laser. Binding of the substrate analogue 4-methylbenzoyl-CoA (4-MBA-CoA) or the substrate itself, 4-CBA-CoA, to the dehalogenase mutants yields a wide variation in the position of the C═O stretching frequency. As can be seen in Table 1 and Figures 3 and 4, it occurs between 1608 and 1669 cm^{-1}. The latter value represents the C═O group in an essentially null electrostatic force environment, being close to 4-bromobenzoyl *S*-alkyl thioester in CCl_4 [with a C═O stretch at 1669 cm^{-1} (*14*)] and 4-methylbenzoyl *S*-ethyl thioester in CCl_4 [C═O stretch at 1663 cm^{-1} (*13*)]. The lowest value is 1608 cm^{-1} for substrate binding to D145A dehalogenase (*15*). The C═O group here is effectively polarized by the hydrogen bonds from the Phe64 and Gly114 backbone NH groups as well as by the positive pole (at Gly114) of the α-helix dipole of residues 114−122. It should be noted that the 4-MBA-CoA does not form an EMc, the electronic properties of the 4-methyl group are unfavorable, and there is no evidence for the characteristic EMc Raman bands near 1510 and 1220 cm^{-1} (*1*, *12*). Thus, in all cases, where we are recording Raman spectra, we are observing the Michaelis complexes.

The mutant enzymes fall into three classes. Changes in A112V and Y65D increase the value of the C═O stretch only modestly over that seen for the WT; changes in G113A and G113S increase the C═O stretch by 30−47 cm^{-1}, and changes at F64P and G113N increase the C═O stretch by ~60 cm^{-1}. The positions of these mutations near the dehalogenase active site are indicated in Figure 2. It is apparent that the position of the C═O frequency can depend on both the position and nature of the site-specific mutation.

The decrease in the C═O frequency is, of course, due to its increasing single-bond character brought about by net electropositive forces near the C═O oxygen. These bring about an increase in the valence bond form II (Scheme 1) to the true structure. As a result, the C═O bond assumes a decrease in double-bond character.

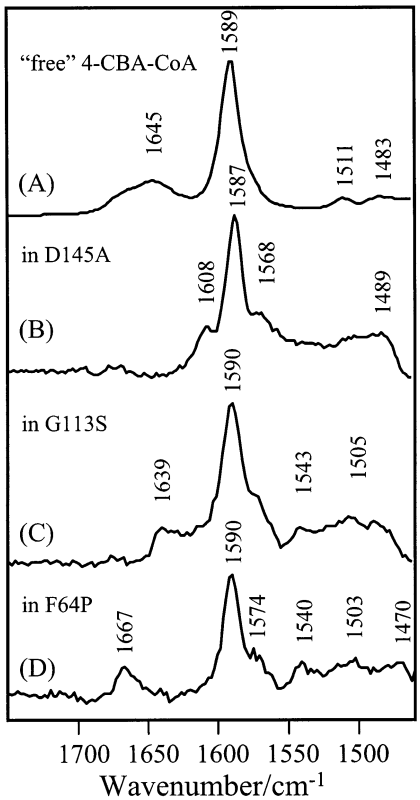

FIGURE 3: Typical Raman spectra of 4-CBA-CoA in various states: (A) free 7.9 mM 4-CBA-CoA in 50 mM Tris-HCl buffer, (B) bound to D145A (392 μM) at an E:S ratio of 1:1, (C) bound to G113S (430 μM) at an E:S ratio of 2:1 (averaged data for the first 15 min), and (D) 4-CBA-CoA bound to F64P (290 μM) at an E:S ratio of 2:1 (the first 5 min of data). All were at pH 7.5 in 50 mM Tris buffer. The band ranging from 1608 to 1667 cm^{-1} is due to the C═O stretching vibration of the thioester group, and the intense band at 1590 and an unresolved shoulder at 1570 cm^{-1} are due to the phenyl ring C═C stretching modes (modes 8a and 8b).

For the WT (or D145A), the two peptide NH hydrogen bonds and the α-helix dipole appear to be oriented to achieve maximal polarization. Although we cannot dissect the polarizing forces into their individual components, we are

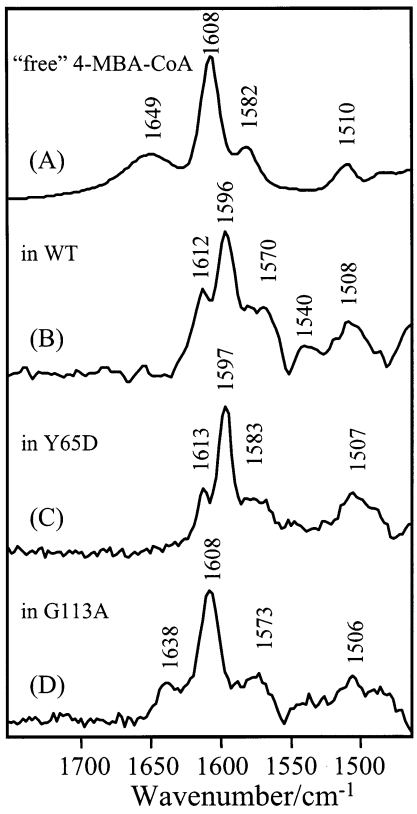

FIGURE 4: Typical Raman spectra of 4-MBA-CoA in various states: (A) free 4-MBA-CoA (4.2 mM) in 50 mM Tris-HCl buffer, (B) 4-MBA-CoA bound to WT enzyme (350 μM) at an E:L ratio of 1:1, (C) 4-MBA-CoA bound to Y65D (200 μM) at an E:L ratio of 1:1, and (D) 4-MBA-CoA bound to G113A (245 μM) at an E:L ratio of 3:2. All were at pH 7.5 in 50 mM Tris-HCl buffer. The band ranging from 1612 to 1638 cm^{-1} is due to the C═O stretching vibration of the thioester group, and the intense band between 1608 and 1596 cm^{-1} and an unresolved shoulder from 1582 to 1570 cm^{-1} are due to the phenyl ring C═C stretching modes (modes 8a and 8b).

Scheme 1

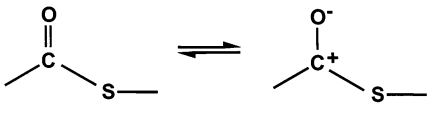

able to estimate the effective hydrogen bonding strength. In this instance, this is defined as the strength of a single hydrogen bond that would shift the C═O stretch from its unperturbed position of 1669 cm^{-1} to its position of 1608 cm^{-1} for the most highly polarized form. The estimate is made by undertaking hydrogen bonding studies on the model compound 4-methylbenzoyl *S*-ethyl thioester in CCl_4 using FTIR spectroscopy. Details are given in the publications by Clarkson et al. (*13*), where it is shown for benzoyl thioesters that the enthalpy of effective hydrogen bonding strength (ΔH) is linearly related to the shift of the C═O stretch frequency ($\Delta\nu_{C=O}$) by the following equation:

$$-\Delta H = 1.24\nu_{C=O} - 8.72 \text{ kJ/mol} \quad (4)$$

For this series of dehalogenase complexes, this gives a change in the effective H-bonding strength of 67 kJ/mol (16 kcal/mol), which is obviously a potent polarizing force at the C═O bond.

Kinetic and Thermodynamic Properties of Site-Directed Mutants. Dehalogenase mutants G63A, G63I, G63P, G115V, G115N, G115L, G115S, and A112G were overexpressed as insoluble proteins and were not pursued further. Dehalogenase mutants G113V and A112S were expressed as soluble proteins; however, upon purification and concentration, the proteins precipitated from solution. These mutant dehalogenases were not examined further. Dehalogenase mutants A112V, G113N, G113S, G113A, Y65D, and F64P were overexpressed as soluble proteins and purified to homogeneity (as determined by SDS−PAGE). Their solubility, wild-type dehalogenase-like chromatographic behavior, and stability were indicative of a native fold.

The steady-state kinetic constants k_{cat} and K_m were determined at 25 °C and pH 7.5 using a continuous spectrophotometric assay. The results are listed in Table 1. The dehalogenase mutants F64P and G113N did not possess sufficient activity for determination of K_m. For these mutants, the k_{cat} was calculated from the initial velocity measured at a presumed saturating level of substrate. The k_{cat} values of the mutants ranged from 0.0013% (7.6×10^{-6} s^{-1}) to 73% (0.44 s^{-1}) of the wild-type dehalogenase k_{cat} value (0.60 s^{-1}). This range was sufficient for exploration of the relationship between the rate of catalysis of formation of the Meisenheimer intermediate and the ability of the enzyme to polarize the substrate or substrate analogue, 4-MBA-CoA, as defined by the C═O stretching frequency. The binding affinities of the mutant dehalogenase for the 4-MBA-CoA ligand were determined by fluorescence titration. The K_d values that were obtained are listed in Table 1. These values ranged from 1.7 to 140 μM compared to the K_d of 1.6 μM measured for the wild-type dehalogenase. The binding affinity of each mutant was strong enough to ensure adequate population of the enzyme−ligand complex for Raman measurement.

The dehalogenase reaction pathway is a multistep one, and each step, including product release, attenuates the turnover rate (*2*). For the wild-type dehalogenase, the rate of a single turnover is 2.3 s^{-1} which is ca. 4-fold faster than the steady-state turnover rate. The k_{obs} for EAr formation (from the ES complex) is 24 s^{-1} (Table 1). Because EAr formation follows EMc formation, 24 s^{-1} is the lower limit for the *k* for EMc formation. In wild-type dehalogenase, the EAr accumulates to a level corresponding to 22% of the bound substrate, while in the A112V mutant, it accumulates to a level of 23% (Figure 5). In the Y65D mutant, the k_{obs} for EAr formation (3.4 s^{-1}) is slower than the k_{obs} for EAr formation in A112V (17 s^{-1}), or in wild-type dehalogenase (24 s^{-1}). Nevertheless, the EAr accumulates to a level of 17% because the rate of EAr hydrolysis is also reduced in this mutant (see Figure 5).

The severely decreased k_{cat} and k_{obs} values (for the single-turnover reaction, Table 1) determined for the F64P, G113A, G113S, and G113N mutants indicate that one or more of the forward microscopic rate constants have been drastically reduced. Because the mutation is directed at the disruption of substrate polarization, it was hypothesized that EMc formation is a limiting step in these mutants. A mutation which inhibits the rate at which EAr is formed to a greater extent than the rate at which it is consumed will preclude the accumulation of the EAr intermediate. Therefore, the precipitated enzyme fractions derived from single-turnover reactions catalyzed by F64P, G113A, G113S, and G113N

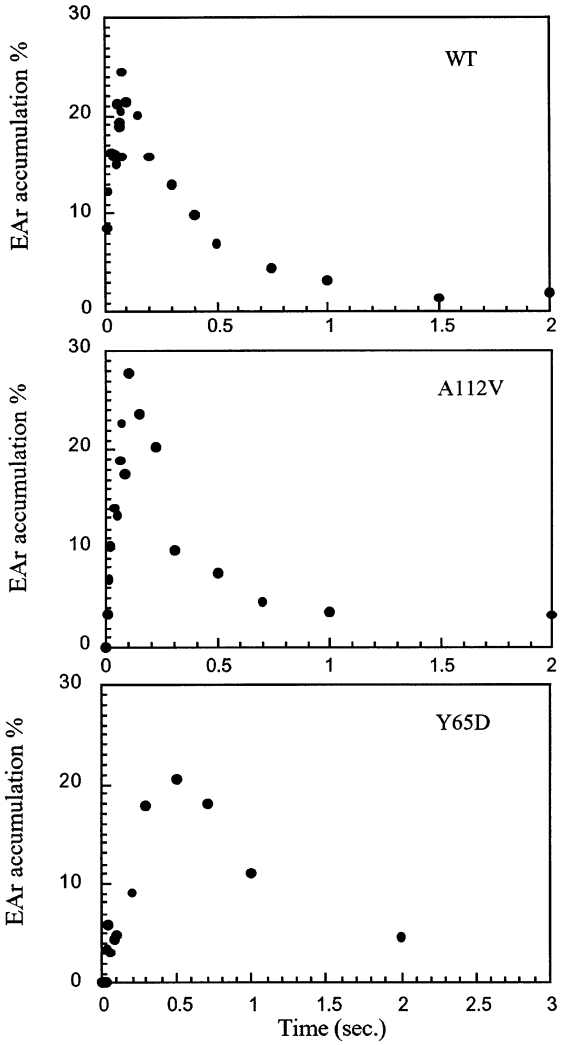

FIGURE 5: Accumulation of EAr in the single-turnover reaction of 115 μM WT dehalogenase with 52 μM 4-CBA-CoA, 144 μM A112V with 66 μM 4-CBA-CoA, and 144 μM Y65D with 66 μM 4-CBA-CoA in 50 mM Hepes buffer (pH 7.5, 25 °C) measured with rapid quench mixing and the spectrophotometric assay at 330 nm.

dehalogenases, and quenched at varying conversions, were analyzed for EAr content. In contrast to wild-type, A112V, and Y65D dehalogenase, the F64P, G113A, G113S, and G113N mutant dehalogenases did not contain a detectable level (>3%) of the EAr intermediate. This result suggests that EAr formation is limiting in these mutants.

Because EAr is formed in two steps, consisting of the conversion of ES to EMc and then EMc to EAr, inhibition of either of these steps could cause EAr formation to become rate-limiting. Therefore, only if it were known (which it is not) that the EMc intermediate is converted to EAr in the quenched reaction could it be known with certainty that the ES to EMc step is rate-limiting in the reaction pathway catalyzed by the mutants. Nevertheless, it is not unreasonable to assume that EMc formation is rate-limiting because the mutation is more likely to impair the stabilization of the transition state leading to the EMc intermediate than it is the transition state associated with the expulsion of the chloride ion from this intermediate. This latter step, which is driven by the gain in aromaticity, occurs without the assistance of active site residues and, thus, is not expected to be sensitive to amino acid replacement made at a distant position in the catalytic site. In contrast, a mutation that reduces the level of H-bond interaction with the substrate benzoyl C═O group should reduce the affinity of the substrate for the enzyme (note the increased K_d values of the mutant enzyme−4-MBA-CoA complexes listed in Table 1) and, to a much greater extent, reduce the extent of stabilization of the charged EMc intermediate (and the transition state leading to it).

DISCUSSION

Polarization throughout the Benzoyl π-Electron System. For a delocalized π-electron system such as the benzoyl moiety, two kinds of polarization effects can be distinguished. In the first, strong electropositive forces near the C═O oxygen increase electron density at the oxygen atom with a consequent increase in C═O single-bond character and a downshift in the stretching frequency. The electron pull at the C═O group is not accompanied by electron release (or push) at the 4 position. Consequently, there is only minor π-electron rearrangement throughout the benzoyl skeleton, and phenyl ring modes are only perturbed modestly. Thus, in this case, the phenyl 8a and 8b modes shift only from 1608 to 1596 cm^{-1} when 4-MBA-CoA binds to WT dehalogenase, although the C═O group undergoes strong local polarization. This situation is accompanied by a fairly small red shift in the benzoyl's $\pi-\pi^*$ transition, typically from 260 to 302 nm upon binding (*12*).

However, when electron release is available at the 4 position, e.g., from the O^- or OH moiety of the bound product 4-HBA-CoA, a synergistic combination of electron "pull" at the C═O group and "push" at the 4 position causes a major rearrangement throughout the entire π-electron system. This leads to the benzenoid ring becoming more quinonoid-like, and the 8a and 8b ring modes are replaced by double-bond features near 1560 and 1525 cm^{-1} in the 4-HBA-CoA−WT enzyme complex (*12*). This effect is accompanied by a major red shift in the $\pi-\pi^*$ transition from 293 to ~370 nm upon binding of the product to the enzyme. Such massive spectral changes were first observed in resonance Raman studies of chromophoric substrates binding to papain (*16*) and later in Raman difference (nonresonance) spectroscopic studies of model substrates binding to cysteine proteases (*17*, *18*). The significance of this second class of polarized systems is that the large rehybridization at the C═O group, brought about by "push-me-pull-you" electronic effects, precludes setting up relationships involving the properties of the carbonyl and reactivity (*19*).

In this instance, we are fortunate that substrate polarization is localized primarily in the C═O group, enabling us to quantitate changes in hydrogen bonding strength with nearby site-specific mutations in the enzyme. However, the consequent changes in electron density transmitted to the 4 position as the reaction proceeds do give rise to the large observed changes in rate of formation of the Meisenheimer complex.

Correlation between the C═O Stretching Frequency and the Rate of Formation of the Meisenheimer Complex. Above, we made the case that the rate-limiting step for the reaction of the substrate with the severely compromised mutants of dehalogenase (G113A, G113S, G113N, and F64P) is the formation of the Meisenheimer complex shown in Figure 1,

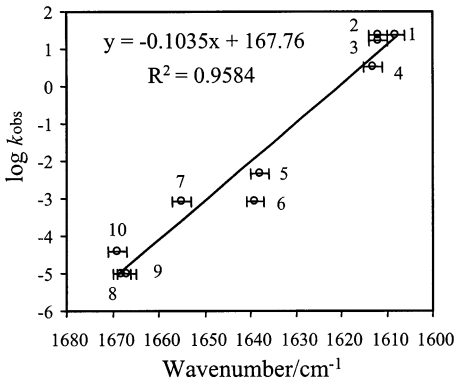

FIGURE 6: Plot of $\nu_{C=O}$ frequencies vs the single-turnover rate (log k_{obs}) for the 4-CBA-CoA dehalogenase series. (1) 4-CBA-CoA−D145A: 1608 cm^{-1}, k_{obs}(WT) = 24 s^{-1}. (2) 4-MBA-CoA−WT: 1612 cm^{-1}, k_{obs} = 24 s^{-1}. (3) 4-MBA-CoA−A112V: 1612 cm^{-1}, k_{obs} = 17 s^{-1}. (4) 4-MBA-CoA−Y65D: 1613 cm^{-1}, k_{obs} = 3.4 s^{-1}. (5) 4-MBA-CoA−G113A: 1638 cm^{-1}, $k_{obs} = 4.5 \times 10^{-3}$ s^{-1}. (6) 4-CBA-CoA−G113S: 1639 cm^{-1}, $k_{obs} = 8.5 \times 10^{-4}$ s^{-1}. (7) 4-MBA-CoA−G113S: 1655 cm^{-1}, $k_{obs} = 8.5 \times 10^{-4}$ s^{-1}. (8) 4-MBA-CoA−F64P: 1668 cm^{-1}, $k_{obs} = 1 \times 10^{-5}$ s^{-1}. (9) 4-CBA-CoA−F64P: 1667 cm^{-1}, $k_{obs} = 1 \times 10^{-5}$ s^{-1}. (10) 4-CBA-CoA−G113N: 1669 cm^{-1}, $k_{obs} = 3.9 \times 10^{-5}$ s^{-1}. The solid line represents a linear regression fit to the data with a correlation coefficient R^2 of 0.9584. The error bars denote the accuracy of C=O frequency positions (2 cm^{-1}).

and that by measuring the values of k_{obs} of EP under single-turnover conditions we are measuring the rate of Meisenheimer formation.

As can be seen in Figure 6, for 10 ligand and enzyme combinations, there is a good correlation between the position of the C=O stretching frequency and k_{obs} (R^2 = 0.9584), where k_{obs} is the rate of formation of EP derived from single-turnover experiments for severely impaired mutants in which EAr does not accumulate (G113A, G113A, G113N, and F64P) or rate of formation of EAr for enzymes in which EAr accumulates (WT, A112V, and Y65D). The ranges are quite broad, and reactivity varies by approximately 2400000-fold and $\nu_{C=O}$ by 61 cm^{-1}. As we have discussed above, the latter translates into a change in effective hydrogen bonding strength (enthalpy) of ~67 kJ/mol. Thus, it appears that modulating the hydrogen bonding strength at the C=O group, by modifying the dispositions of the two H-bond donors and the electrostatic potential due to the α-helix dipole, affects the transition state for formation of the Meisenheimer complex five chemical bonds away. Moreover, there appears to be a good correlation between the enthalpy of the effective hydrogen bonding strength and log k_{obs}. By using the relationship

$$\Delta G = -RT \ln[(k_{obs}h)/(kT)] \quad (5)$$

we find that the difference in ΔG values ($\Delta\Delta G$) for the series of complexes in Figure 6 is 36 kJ/mol. Thus, we can conclude that approximately half of the enthalpy available with the increase in the polarizing forces at the substrate's C=O group finds use in reducing the free energy between the ground and transition states for Meisenheimer formation. In this, we have made the assumption that entropy factors are changed little going through the series of enzyme−ligand complexes shown in Figure 6 and Table 1.

There is a remarkable correspondence between the results displayed in Figure 6 for the system presented here and the

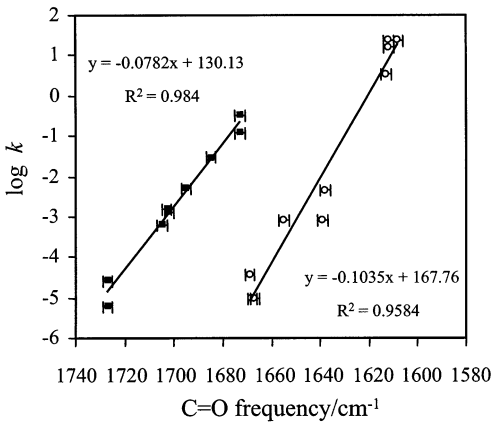

FIGURE 7: Correlation between carbonyl stretching frequencies and log k in two enzyme systems. Empty circles correspond to data for the 4-CBA-CoA dehalogenase series in this study (see Figure 6). Data for the serine protease series are shown as filled squares. The data of $\nu_{C=O}$ stretching frequencies and the deacylation rates log k_3 in the acyl serine protease are taken from ref *21*. The solid lines represent linear regression fits to the data of each series (a correlation coefficient R^2 of 0.984 was obtained in the acyl serine protease). The error bars denote the accuracy of C=O positions (±2 cm^{-1}).

Chart 1: Acyl Enzyme Intermediate in Serine Protease, Represented by Chymotrypsin

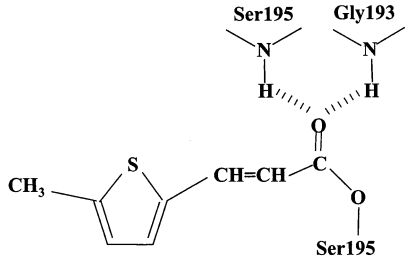

results we obtained for the deacylation of a series of acyl enzymes involving subtilisin and chymotrypsin (*20*, *21*). In the latter studies, because of technical limitations, we had to use chromophoric substrates to generate resonance Raman spectra possessing sufficient intensity to permit detection. Thus, the acyl enzymes were of the form shown in Chart 1. The resonance Raman spectra were measured in a flow system for the fully active species following a pH jump. The pH jump leads to the base-catalyzed onset of deacylation, but the spectral data were acquired before significant deacylation had occurred. The results for a series of acyl enzymes, showing the C=O stretching frequencies and the logarithms of the deacylation rate constant, log k_3, are shown in Figure 7. The results yield a very well-defined straight line (R^2 = 0.984). The implications of these findings have been widely discussed in the literature in terms of the relationships among the reactivity, the effective hydrogen bonding strength at the acyl C=O group, and the changes in the C=O bond length throughout the series (*21*−*23*). Here, we note the strong similarities between the findings for the acyl-serine proteases and the series of dehalogenase complexes. Figure 7 compares the two sets of data. For the serine protease complexes, reactivities vary by 16300-fold and C=O stretching frequencies by 54 cm^{-1}. For the dehalogenases, reactivities vary by ~2400000-fold and C=O stretching frequencies by 61 cm^{-1}. The slopes of the two plots of $\nu_{C=O}$ versus log k are similar. Moreover, two sets of experiments probing hydrogen strengths for model compounds show that

for the serine proteases the change in the C═O stretch of 54 cm^{-1} is equivalent to a change in the effective hydrogen bonding strength of 57 kJ/mol (*24*), whereas for the dehalogenase series, the change in the C═O stretch of 61 cm^{-1} is equivalent to a change in the effective hydrogen bonding strength of 67 kJ/mol (*13*).

Thus, for both series of enzymatic reactions, the effect of hydrogen bonding (and dipole) interactions at a C═O group appear to be correlated with rate acceleration. Moreover, there is quite good quantitative agreement. We define a value $\log_{10} \kappa/\Delta H$, where κ is the ratio of the fastest and slowest rate constants and ΔH is the corresponding difference in effective hydrogen bonding strength across the series (this is akin to the slopes seen in Figure 7). This gives the log of rate acceleration generated per kilojoule per mole of H-bond strength. It is 0.074 for the acyl enzyme series and 0.095 for the dehalogenase series. This finding tells us that a similar change in the effective H-bond interaction at the C═O group is associated with a similar degree of rate acceleration in both reactions. Of course, the latter represents a difference in ground-state and transition-state energies, while the interactions at the C═O group are assessed solely in the ground state. Nevertheless, it seems remarkable that a similar relationship between $\nu_{C=O}$ (or ΔH) and log k holds for the nucleophilic substitution seen directly at the acyl carbonyl, for the acyl enzymes, and for the interaction at the thioester carbonyl and nucleophilic aromatic addition occurring five bonds away in a delocalized π-electron system bound in the active site of dehalogenases.

REFERENCES

1. Dong, J., Carey, P. R., Wei, Y., Luo, L., Lu, X., Liu, R.-Q., and Dunaway-Mariano, D. (2002) *Biochemistry 41*, 7453−7463.
2. Zhang, W., Wei, Y., Luo, L., Taylor, K. L., Yang, G., Dunaway-Mariano, D., Benning, M. M., and Holden, H. M. (2001) *Biochemistry 40*, 13474−13482.
3. Benning, M. M., Taylor, K. L., Liu, R. Q., Yang, G., Xiang, H., Wesenberg, G., Dunaway-Mariano, D., and Holden, H. M. (1996) *Biochemistry 35*, 8103−8109.
4. Luo, L., Taylor, K. L., Xiang, H., Wei, Y., Zhang, W., and Dunaway-Mariano, D. (2001) *Biochemistry 40*, 15684−15692.
5. Dong, J., Luo, L., Liang, P.-H., Dunaway-Mariano, D., and Carey, P. R. (2000) *J. Raman Spectrosc. 31*, 365−371.
6. Carey, P. R., and Tonge, P. J. (1995) *Acc. Chem. Res. 28*, 8−13.
7. Liang, P.-H., Yang, G., and Dunaway-Mariano, D. (1993) *Biochemistry 32*, 12245−12250.
8. Chang, K. H., Liang, P. H., Beck, W., Scholten, J. D., and Dunaway-Mariano, D. (1992) *Biochemistry 31*, 5605−5610.
9. Bradford, M. (1976) *Anal. Biochem. 72*, 248−254.
10. Anderson, K. S., Sikorski, J. A., and Johnson, K. A. (1988) *Biochemistry 27*, 7395−7406.
11. Dong, J., Xiang, H., Luo, L., Dunaway-Mariano, D., and Carey, P. R. (1999) *Biochemistry 38*, 4198−4206.
12. Taylor, K. L., Liu, R. Q., Liang, P. H., Price, J., Dunaway-Mariano, D., Tonge, P. J., Clarkson, J., and Carey, P. R. (1995) *Biochemistry 34*, 13881−13888.
13. Clarkson, J., Tonge, P. J., Taylor, K. L., Dunaway-Mariano, D., and Carey, P. R. (1997) *Biochemistry 36*, 10192−10199.
14. Nyquist, R. A., and Potts, W. J. (1959) *Spectrochim. Acta 7*, 514−538.
15. Hong, X., Dong, J., Dunaway-Mariano, D., and Carey, P. R. (1999) *Biochemistry 38*, 4207−4213.
16. Carey, P. R., Carriere, R. G., Lynn, K. R., and Schneider, H. (1976) *Biochemistry 15*, 2387−2393.
17. Dinakarpandian, D., Shenoy, B., Pusztai-Carey, M., Malcolm, B. A., and Carey, P. R. (1997) *Biochemistry 36*, 4943−4948.
18. Dinakarpandian, D., Shenoy, B. C., Hilvert, D., McRee, D. E., McTigue, M., and Carey, P. R. (1999) *Biochemistry 38*, 6659−6667.
19. Doran, J., Tonge, P. J., Mort, J. S., and Carey, P. R. (1996) *Biochemistry 35*, 12487−12494.
20. Tonge, P. J., and Carey, P. R. (1990) *Biochemistry 29*, 10723−10727.
21. Tonge, J., and Carey, P. R. (1992) *Biochemistry 31*, 9122−9125.
22. Fersht, A. (1998) *Structure and Mechanism in Protein Science, A Guide to Enzyme Catalysis and Protein Folding*, Chapter 16, p 476, W. H. Freeman, New York.
23. Cannon, W. R., Singleton, S. F., and Benkovic, S. J. (1996) *Nat. Struct. Biol. 3*, 821−833.
24. Tonge, P. J., Fausto, R., and Carey, P. R. (1996) *J. Mol. Struct. 379*, 135−142.

BI0347656